Physical Explanation of the H_0-Tension

Hans-Otto Carmesin[1,2,3]

[1]*(University Bremen, Germany)*
[2]*(Studienseminar Stade, Germany)*
[3]*(Observatory and Gymnasium Athenaeum Stade, Germany)*

ABSTRACT: *Various observations of the Hubble constant H_0 provide different values. That problem is called H_0-tension. Here a physical explanation of the H_0-tension is provided: Each observed value depends on the time or redshift of the emission of the used probe, as a consequence of the time evolution of the universe. This causes a large increase of H_0 in the late universe. Moreover, the under-density at the local universe causes a small decrease of H_0. A quantum gravity theory of dark energy is in precise accordance with observation. Thereby, no fit is executed, of course.*

KEYWORDS − *cosmology, dark energy, quantum gravity, relativity, structure formation*

I.   INTRODUCTION

The expansion of the universe since the Big Bang is characterized by an **expansion rate**, described by the Hubble parameter H(z). It is a function of the redshift z. In particular, the value of H at the present time t_0 is called Hubble parameter $H_0 = H(t_0)$ (see e. g. [1]). The measurement of the Hubble constant H_0 exhibits a problem: Various observers achieve different values of H_0 (see e. g. [2-12]). That problem is called **H_0-tension** or Hubble tension (see e. g. [2, 4, 13]). The purpose of the present paper is to **provide a physical explanation** of the H_0-tension. Especially relevant contributions of the present paper include the following results:

Firstly and in general, the observed values $H_{0,obs}$ of the Hubble constant H_0 are explained by the fact that each observation is based on a probe emitted at a respective redshift z and at a corresponding local density of matter $\rho_{m,L}$ of the local universe:

$$H_{0,obs} = H_{0,obs}(z, \rho_{m,L}) \tag{1}$$

Secondly and in particular, the above function (see equation 1) can be expressed by a reference value $H_{0,ref}$ multiplied by two correction factors $Q_z(z)$ and $Q_m(\rho_{m,L})$:

$$H_{0,obs} = H_{0,ref} \cdot Q_z(z) \cdot Q_m(\rho_{m,L}) \tag{2}$$

Thirdly, the observed values $H_{0,obs}$ [2-12] are physically explained with help of a theory that has been derived from basic physical principles only (see e. g. [14-19]), whereby no fit procedure has been applied (see e. g. [18]).

II.   USED OBSERVATIONS OF LOCAL DENSITIES

In this section, we summarize observations of local densities of matter $\rho_{m,local}$ in the vicinity of our galaxy, the Milky Way. For comparison, we apply the mean density of matter of the universe ρ_m. It has been derived from observations of the CMB (see [2] and Table 15.2 in [16]):

$$\rho_m = 2.73 \cdot 10^{-27} \frac{kg}{m^3} \tag{3}$$

Secondly, we investigate the local basin of attraction that includes the Milky Way: Laniakea (see [20, 21]). A corresponding estimation of the radius r_{Lan} of Laniakea is as follows [20,22]:

$$r_{Lan} = \frac{80 \, Mpc}{h} \quad with \quad h = \frac{H_0}{100 \frac{km}{s \cdot Mpc}} = 0.6736 \quad or \quad r_{Lan} = 3.67 \cdot 10^{24} \, m \tag{4}$$

Probes emitted at that radius r_{Lan} exhibit the following redshift:

$$z_{Lan} = 0.028 \tag{5}$$

An estimate of the density of matter of Laniakea $\rho_{m,Lan}$ amounts to 94 % of ρ_m (see section 3.2 in [22]):

$$\rho_{m,Lan} = 0.94 \cdot \rho_m = 2.57 \cdot 10^{-27} \frac{kg}{m^3} \tag{6}$$

Thirdly, we summarize a larger region that includes the Milky Way. It has been found by the REFLEX II survey and it exhibits an under-density of 15 % [23]:

$$\rho_{m,RII} = 0.85 \cdot \rho_m = 2.32 \cdot 10^{-27} \frac{kg}{m^3} \tag{7}$$

That region has the following radius r_{RII} [23]:

$$r_{RII} = 170 \, Mpc = 5.25 \cdot 10^{24} \, m \tag{8}$$

Probes emitted at that radius r_{RII} exhibit the following redshift:

$$z_{II} = 0.04 \tag{9}$$

Moreover, that survey shows that there is no significant under-density at balls with the center at the Milky Way and with a radius larger than r_{RII}.

III.   USED REFERENCE VALUE FOR H₀

In this section, we summarize the choice of the reference value $H_{0,ref}$ and the corresponding results. In principle, the reference value $H_{0,ref}$ for H_0 can be chosen at any redshift z. In order to obtain a reference value that is relatively independent of the local density, we choose the value of H_0 at the redshift of the emission of the cosmic microwave background, CMB. The corresponding redshift is $z_{CMB} = 1089.92 \pm 0.25$ and the respective value of the Hubble constant is as follows (see [2], Table 2):

$$H_{0,ref} = 67.36 \pm 0.54 \, \frac{km}{s \cdot Mpc} = H_0(z_{CMB}) \tag{10}$$

IV.   DERIVATION OF THE CORRECTION FACTOR FOR THE LOCAL DENSITY

In this section, we derive the correction factor $Q_m(\rho_{m,local})$ describing the effect of the local density of matter $\rho_{m,local}$ at the emission of the probe used in an observation of the Hubble constant H_0. For it we apply the general equation for the Hubble parameter (see e. g. [1]):

$$H^2 = \frac{8\pi \cdot G}{3} \cdot \rho \tag{11}$$

Hereby, we applied the fact that the curvature parameter is zero (see e. g. [1] or theorem 32(6) in [16]). In general, we mark a local quantity by the subscript L, whereas a variable describing a spatial average or a homogeneous quantity or a global quantity is not marked by a subscript. In particular, for the case of the present time, the density ρ in equation (4) takes its present day value ρ_0. Moreover, the density ρ is the sum of the density of matter ρ_m, of the density of radiation ρ_r and of the density of dark energy ρ_Λ (see e. g. [1] or [16]). So the Hubble constant H_0 obeys the following equation:

$$H_0{}^2 = \frac{8\pi \cdot G}{3} \cdot \rho_0 = \frac{8\pi \cdot G}{3} \cdot (\rho_{m,0} + \rho_{r,0} + \rho_{\Lambda,0}) \tag{12}$$

If an observation of H_0 is based on a probe that is emitted at a local density of matter $\rho_{m,L}$ and that propagates through an area with that density, then the observed Hubble constant $H_{0,obs}$ is characterized by equation (12), whereby the density of matter $\rho_{m,0}$ is replaced by the local density of matter $\rho_{m,L}$:

$$H_0{}^2(\rho_{m,L}) = \frac{8\pi \cdot G}{3} \cdot (\rho_{m,L} + \rho_{r,0} + \rho_{\Lambda,0}) \tag{13}$$

Correspondingly, the correction factor $Q_m(\rho_{m,L})$ is defined by the ratio $H_0(\rho_{m,L})$ and H_0:

$$Q_m(\rho_{m,L}) = \frac{H_0(\rho_{m,L})}{H_{0,ref}} = \sqrt{\frac{\rho_{m,L}}{\rho_0} + \frac{\rho_{r,0}}{\rho_0} + \frac{\rho_{\Lambda,0}}{\rho_0}} \tag{14}$$

The densities $\rho_{r,0}$ and $\rho_{\Lambda,0}$ are scaled by ρ_0 in order to obtain the density parameters (see [2] or [18]):

$$\Omega_r = \frac{\rho_{r,0}}{\rho_0} = 9.265 \cdot 10^{-5} \quad and \quad \Omega_r = \frac{\rho_{\Lambda,0}}{\rho_0} = 0.6847 \tag{15}$$

In particular, for the case of a probe emitted within a ball with the center at the Milky Way and with a density $\rho_{m,L}$, the correction factor is as follows:

$$Q_m(\rho_{m,L}) = \sqrt{\frac{\rho_{m,L}}{\rho_0} + \Omega_r + \Omega_\Lambda} \tag{16}$$

According to equation (7), the correction factor at the region with radius r_{RII} is as follows:

$$Q_m(\rho_{m,L}) = 0.976 \tag{17}$$

Correspondingly, the difference $\Delta H_0(\rho_{m,L}) = H_0 \cdot (Q_m(\rho_{m,L}) - 1)$ is as follows:

$$\Delta H_0(\rho_{m,L}) = -1.75 \frac{km}{s \cdot Mpc} \quad for \quad z \in [0, 0.04] \tag{18}$$

The H_0 value in Fig. 1 marked by a full square (■) is based on a sample of probes ranging from $z = 0.023$ until $z = 0.15$ (see [4, 12]). So the difference $\Delta H_0(\rho_{m,L})$ has to be applied in a partial manner. For it, the difference $\Delta H_0(\rho_{m,L})$ in equation 18 is applied to probes in the interval $z \in [0.023, 0.04]$, whereas the difference $\Delta H_0(\rho_{m,L}) = 0$ is applied to probes in the interval $z \in [0.04, 0.15]$ in a manner proportional to the size of these intervals as follows:

$$\Delta H_{0,partial}(\rho_{m,L}) = \frac{0.017}{0.127} \cdot \left(-1.75 \frac{km}{s \cdot Mpc}\right) + \frac{0.11}{0.127} \cdot 0 \frac{km}{s \cdot Mpc} = -0.23 \frac{km}{s \cdot Mpc} \tag{19}$$

Each observed value $H_{0,obs}$ can be transformed to a **global observation value** $H_{0,obs,global}$ by subtracting the difference $\Delta H_0(\rho_{m,L})$ describing the effect of the local universe (see equations 18 and 19):

$$H_{0,obs,global}(z) = H_{0,obs} - \Delta H_{0,partial}(\rho_{m,L}) \cdot \Theta(0.04 - z) \tag{20}$$

Hereby, $\Theta(x)$ represents the Heavyside function. Thereby, $\Theta(x) = 0$ for $x < 0$ and $\Theta(x) = 1$ for $x \geq 0$. In particular, for the case of the megamaser probe in Fig. 1, the global observation value is determined as follows:

$$H_{0,obs} = 73.9 \frac{km}{s \cdot Mpc} \quad and \quad z = 2 \cdot 10^{-5} \quad \rightarrow \quad H_{0,obs,global} = 75.65 \frac{km}{s \cdot Mpc} \tag{21}$$

Similarly, for the case of the surface brightness probe in Fig. 1, the global observation value is as follows:

$$H_{0,obs} = 73.3 \frac{km}{s \cdot Mpc} \quad and \quad z = 1.7 \cdot 10^{-5} \quad \rightarrow \quad H_{0,obs,global} = 75.05 \frac{km}{s \cdot Mpc} \qquad (22)$$

Analogously, the distance ladder probe at small z (see ■ in Fig. 1) is transformed as follows:

$$H_{0,obs} = 73.2 \frac{km}{s \cdot Mpc} \quad and \quad z \in [0.023, 0.15] \quad \rightarrow \quad H_{0,obs,global} = 73.43 \frac{km}{s \cdot Mpc} \qquad (23)$$

The other probes in Fig. 1 essentially correspond to redshifts above 0.04, thus their global observation values are equal to their respective observed values:

$$H_{0,obs,global} = H_{0,obs} \qquad for \quad z > 0.04 \qquad (24)$$

V.   USED CORRECTION FACTOR FOR THE REDSHIFT

In this section, we summarize the application of a semiclassical theory and of a more general quantum theory (see e. g. [17]) to the derivation of the correction factor $Q_z(z)$ in equation 2. That correction factor $Q_z(z)$ describes the global effect of the redshift z on the observed values $H_{0,obs}$. That means, all local effects on $H_{0,obs}$ are included in the other correction factor $Q_m(\rho_{m,L})$ in equation 2. The global dependence of z on $H_{0,obs}$ is a consequence of the fact that the density of the dark energy ρ_Λ depends slightly on the redshift z, as shown in my quantum gravity theory (see e. g. [14-19]). The corresponding function $\rho_\Lambda(z)$ is applied to the basic equation 11:

$$Q_z(z) = \sqrt{\Omega_m + \Omega_r + \frac{\rho_\Lambda(z)}{\rho_0}} \qquad (19)$$

The ratio in the above equation has been derived for the case of a semiclassical theory as follows. Firstly, an additional term κ(z) is defined as follows (see theorem 22(2a) in [16]):

$$\kappa(z) = \frac{\Omega_m(z_{CMB})}{\Omega_\Lambda(z_{CMB})} \cdot \sigma_8 \cdot \frac{9}{20} \cdot \frac{1}{(1+z)^2} \quad with \quad \sigma_8 = 0.8111 \qquad (20)$$

Hereby, σ_8 is the amplitude of matter fluctuations (see e. g. [16]), and the value 0.8111 has been obtained on the basis of the observation of the CMB [2]. Secondly, within the semiclassical theory, the density of the dark energy is as follows (see theorem 22(2b) in [16]):

$$\rho_\Lambda(z) = \frac{c^2}{4\pi \cdot G \cdot R_H^2} \cdot \left(1 + \kappa(z)\right)^2 \quad with \quad R_H = \frac{c}{H_0(z_{CMB})} \qquad (21)$$

Thereby, R_H is the Hubble radius (see e. g. equation 6.68 in [16]) and G represents the gravitational constant. In addition, the density of the dark energy $\rho_\Lambda(z)$ has been derived in the framework of quantum gravity (see e. g. [16-18]). The corresponding result is presented in Fig. 1 in the present paper.
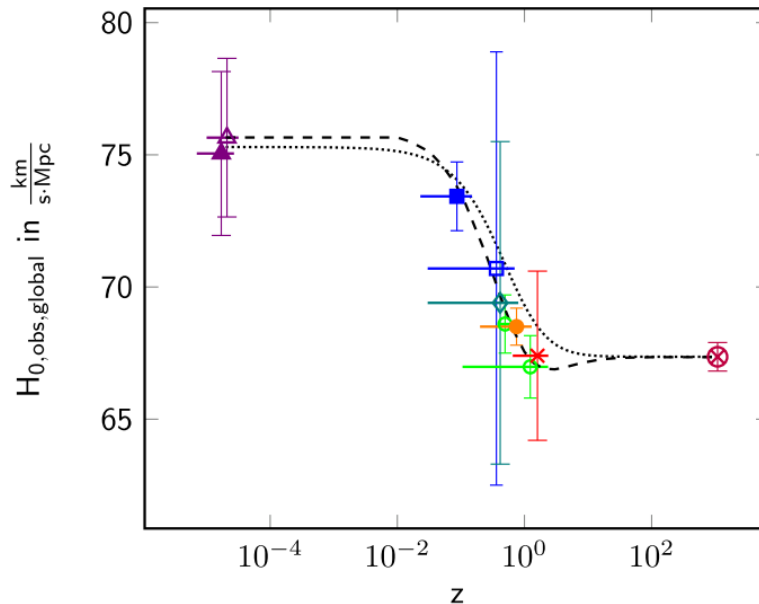
Fig. 1: Observed global Hubble constant H₀,obs,global as a function of the redshift z:

Probes: Δ megamaser [3], ▲ surface brightness [10],
distance ladder at: ■ small z [4, 12], □ large z [11, 19],
◇ gravitational wave [9], o baryonic acoustic oscillations [5, 6],
● weak gravitational lensing and galaxy clustering [7], × strong gravitational lensing [8], ⊗ CMB [2].
Local under-density is applied to data of Δ, ▲ and ■ [20-23].
Theory: ...... semiclassical, - - - - - quantum gravity.

VI. PHYSICAL EXPLANATION OF THE H_0-TENSION

In this section, we apply the above results in order to explain the H_0-tension. For it we present observational and theoretical values of H_0 as a function of the redshift z in Fig. 1. Next we derive further insights from that Fig.

Firstly, the dotted graph in Fig. 1 shows that the H_0 values increase from $H_0(z_{CMB}) = 67.36 \frac{km}{s \cdot Mpc}$ at the early universe to $H_0(z < 0.01) \approx 75 \frac{km}{s \cdot Mpc}$ in the late universe. Hence the largest change of H_0 values is caused by the time evolution of the universe as follows:

$$\Delta H_0(z) \approx 7.6 \frac{km}{s \cdot Mpc} \tag{22}$$

Secondly, we realize that this time evolution of the H_0 values is caused by the time evolution of the density $\rho_\Lambda(z)$ dark energy (see equations 19-21).

Thirdly, we find out that the local under-density of our local universe causes a smaller change of H_0 values as follows (see equations 18-19):

$$|\Delta H_0(\rho_{m,L})| \leq 1.75 \frac{km}{s \cdot Mpc} \tag{23}$$

Fourthly, realize that the local under-density gives rise to a negative change of the H_0 values, as an under-density causes a relatively small density of matter, which in turn causes a relatively small rate of expansion according to the basic equation 11. Note that Turner found out empirically that local under-densities correlate to an increase of H_0 values [24]. Now we explain that empirical observation physically: In the late universe, the time evolution of the density of the dark energy $\rho_\Lambda(z)$ causes relatively large H_0 values (see equations 19-22). Hence these large $H_0(z)$ values observed on the basis of probes of the late universe **correlate to the under-density, but are not caused by that under-density**.

Fifthly, as the concept of the Hubble constant H_0 is a global concept, it makes sense to correct the effect of the under-density. This is achieved by adding $\Delta H_0(\rho_{m,L}) = -1.75 \frac{km}{s \cdot Mpc}$ for all observations based on probes emitted at z less or equal to 0.04 (see equation 18). In particular, the observation based on megamasers (× in Fig. 1) and the observation based on the surface brightness fluctuations of galaxies (□ in Fig. 1) are supplemented by adding $\Delta H_0(\rho_{m,L}) = -1.75 \frac{km}{s \cdot Mpc}$, and the observation based on the cosmic distance ladder and on supernovae at small redshifts (upper ⋆ in Fig. 1) is supplemented by adding $\Delta H_0(\rho_{m,L}) = -0.23 \frac{km}{s \cdot Mpc}$ (see equation 19).

Sixthly, most observations in Fig. 1 are in precise accordance with the semiclassical theory (see dotted graph in Fig. 1). That means that the theoretical H_0 value is within the error of observation.

Seventhly, all observations in Fig. 1 are in precise accordance with the quantum gravity theory (see dashed graph in Fig. 1), as these theoretical H_0 values are within the error of observation.

Eighthly, we realize that the H_0 values exhibit a slight local minimum at z ≈ 1. And this minimum corresponds to a local minimum of the density of the dark energy $\rho_\Lambda(z)$. For details about the physics of that minimum see [14-18].

Ninthly, we realize that the theory underlying the dotted and dashed graphs in Fig. 1 do not execute any fit. Instead, that theory is based on quantum gravity only. In particular, the only numerical input used in that theory is constituted by the present time t_0 after the Big Bang and by the four universal constants of quantum gravity: the gravitational constant G, the velocity of light c, the Boltzmann constant k_B and the Planck constant h (see [18]). Thus the H_0 – tension provides a convincing test of that theory (see Fig. 1).

VII. CONCLUSION

The H_0 – tension is an interesting phenomenon. Moreover, that problem is especially meaningful, since theories of dark energy can be tested with it. In particular, the Fig. 1 provides a convincing positive test of the theory of quantum gravity underlying the dotted and dashed graphs in that Fig. 1 (see [14-18]).

Moreover, that theory of quantum gravity yields a detailed physical explanation of the H_0 – tension: During the time evolution of the universe, the emitted probes exhibit decreasing present day redshifts. Simultaneously, the density of the dark energy exhibits a slight minimum at z ≈ 1 and increases significantly at small redshifts. Thus that density causes a large increase of the observed H_0 values for probes emitted at the late universe. Moreover, probes emitted in the late universe are additionally emitted in the local universe. Hence such probes experience the slight under-density existing in the vicinity of the Milky Way. Thence the H_0 values observed by using such probes exhibit an additional small negative change of the H_0 value.

Altogether, the H_0 – tension is caused by two circumstances: the relatively small local density of matter $\rho_{m,local}$ in the vicinity of the Milky Way and the time evolution of the density of the dark energy $\rho_\Lambda(z)$. Correspondingly, the H_0 – tension can test both circumstances in a quantitative manner. Thereby, the time dependence of the dark energy is the dominating effect, and thus the H_0 – tension is especially suited as a

quantitative test of the time evolution of the dark energy. As a result of these tests, we conclude that the theory applied here is in precise accordance with observation. Thereby that theory is based on quantum gravity only and applies no fit at all.

ACKNOWLEDGEMENTS

REFERENCES

[1]. M. Tanabashi et al. (Particle Data Group), Review of particle physics, *Physical Review D, 98(3),* 2018, 1-1898.
[2]. G. Efstathiou et al. (Planck Collaboration), Planck 2018 results VI. Cosmological parameters, *Astronomy and Astrophysics, 641(A6),* 2020, 1-67.
[3]. D. W. Pesce et al., The megamaser cosmology project: XIII. Combined Hubble constant constraints, *Astrophysical Journal Letters, 891,* 2020, L1.
[4]. A. G. Riess, et al., Cosmic Distances Calibrated at 1 % Precision with Gaia EDR3 Parallaxes and Hubble Space Telescope Photometry of 75 Milky Way Cepheids Confirm Tension with ΛCDM, *The Astrophysical Journal Letters, 908(L6)*, 2021, 1-11.
[5]. O. Philcox, M. Ivanov, M. Simonovic and M. Zaldarriaga, Combining Full-Shape and BAO Analyses of Galaxy Power Spectra: A 1.6 % CMB-Independent Constraint on H$_0$, *arXiv, 2002.04035v3*, 2020, 1-42.
[6]. G. E. Addison, D. J. Watts, C. L. Bennett, M. Halperin, G. Hinshaw, J. L. Weiland, Elucidating ΛCDM: Impact of Baryon Acoustic Oscillation Measurements on the Hubble Constant Discrepancy, *ApJ, 853(2)*, 2018, 1-12.
[7]. T. M. C. Abbott, et al., Dark Energy Survey Year 1 Results: Cosmological Constraints from Galaxy Clustering and Weak Lensing, *Phys. Rev. D, 102*, 2020, 1-34.
[8]. S. Birrer, et al. TDCOSMO: IV. Hierarchical time-delay cosmography - joint inference of the Hubble constant and galaxy density profiles. *Astronomy and Astrophysics, 643*, 2020, 1-40.
[9]. C. Escamilla-Rivera and A. Najera, Dynamical dark energy models in the light of gravitational-wave transient catalogues, *arXiv, 2103.02097v1,* 2021, 1-25.
[10]. J. P. Blakeslee et al., The Hubble Constant from Infrared Surface Brightness Fluctuation Distances, *The Astrophysical Journal, 911(65)*, 2021, 1-12.
[11]. N. Suzuki, et al., The Hubble Space Telescope Cluster Supernova Survey: V. Improving the Dark Energy Constraints above z > 1 and Building an Early-Type-Hosted Supernova Sample, *ApJ, 746,* 2011, 85-105.
[12]. A. G. Riess et al., A 2.4 % Determination of the Local Value of the Hubble Constant, *The Astrophysical Journal, 826(1),* 2016, 1-65.
[13]. E. Di Valentino, et al., In the realm of the Hubble tension - a review of solutions, *Class. Quantum Grav., 38*, 2021, 1-110.
[14]. H.-O. Carmesin, *Entstehung dunkler Energie durch Quantengravitation – Universal Model for Dynamics of Space, Dark Matter and Dark Energy* (Berlin: Verlag Dr. Köster, 2018).
[15]. H.-O. Carmesin, *Entstehung der Raumzeit durch Quantengravitation – Theory for the Emergence of Space, Dark Matter, Dark Energy and Space-Time* (Berlin: Verlag Dr. Köster, 2018).
[16]. H.-O. Carmesin, *Die Grundschwingungen des Universums – The Cosmic Unification* (Berlin: Verlag Dr. Köster, 2019).
[17]. H.-O. Carmesin, *Quanta of Spacetime Explain Observations, Dark Energy, Gravitation and Nonlocality* (Berlin: Verlag Dr. Köster, 2021).
[18]. H.-O. Carmesin, *Cosmological and Elementary Particles Explained by Quantum Gravity* (Berlin: Verlag Dr. Köster, 2021).
[19]. H.-O. Carmesin, *Modeling of SN1a data with my theory* (URL: https://www.researchgate.net/publication/351093848_H0_20 210424pdf#fullTextFileContent, 2021).
[20]. R. B. Tully, H. Courtois, Y. Hoffmann and D. Pomerede, The Laniakea supercluster of galaxies, *Nature, 513(7516),* 2014, 71-74.
[21]. A. Dupuy et al., Partitioning the Universe into gravitational basins using the cosmic velocity field, *MNRAS, 489,* 2019, L1-L6.
[22]. G. Chon and H. Böhringer and S. Zaroubi, On the definition of superclusters, *Astronomy and Astrophysics, L14*, 2015, 1-5.
[23]. H. Böhringer, G. Chon, M. Bristow and C. A. Collins, The extended ROSAT-ESO Flux-Limited X-Ray Galaxy Cluster Survey (REFLEX II), *Astronomy and Astrophysics, 574(A26),* 2015, 1-8.
[24]. E. L. Turner, R. Cen and J. P. Ostriker, The relation of local measures of Hubble's constant to its global value, *The Astronomical Journal, 103(5),* 1992, 1427-1437.